

# Hallmarks of Spin Textures for High-Harmonic Generation

F. Gabriele,<sup>1</sup> C. Ortix,<sup>2,1</sup> M. Cuoco,<sup>1</sup> and F. Forte<sup>1</sup>

<sup>1</sup>*CNR-SPIN, c/o Università di Salerno, IT-84084 Fisciano (SA), Italy*

<sup>2</sup>*Dipartimento di Fisica "E. R. Caianiello", Università di Salerno, IT-84084 Fisciano (SA), Italy*

Spin-orbit coupling and quantum geometry are fundamental aspects in modern condensed matter physics, with their primary manifestations in momentum space being spin textures and Berry curvature. In this work, we investigate their interplay with high-harmonic generation (HHG) in two-dimensional non-centrosymmetric materials, with an emphasis on even-order harmonics. Our analysis reveals that the emergence of finite even-order harmonics necessarily requires a broken twofold rotational symmetry in the spin texture, as well as a non-trivial Berry curvature in systems with time-reversal invariance. This symmetry breaking can arise across various degrees of freedom and impact both spin textures and optical response via spin-orbit interactions. These findings underscore the potential of HHG as a powerful tool for exploring electronic phases with broken rotational symmetry, as well as the associated phase transitions in two-dimensional materials. This approach provides novel perspectives for designing symmetry-dependent nonlinear optical phenomena.

*Introduction* — Recent technological advances in laser science have enabled the development of high-intensity light sources across a wide range of energies. Such strong pulses have been increasingly employed in experimental condensed matter physics to induce nonlinear optical responses in crystalline solids. A notable example is high-harmonic generation (HHG), a nonlinear process in which a material exposed to light at a specific frequency emits radiation at multiples of this fundamental frequency[1, 2]. A key distinction in solid-state HHG is that odd-order harmonics are universally present, whereas even-order harmonics are suppressed by inversion symmetry. Surface, interfaces and certain two-dimensional (2D) materials where inversion symmetry is naturally broken offer potential avenues for observing even-order harmonic emission. 2D non-centrosymmetric structures of materials with substantial spin-orbit coupling (SOC) are generally characterized by a finite Rashba SOC[3, 4]. This leads to energy band splitting and the emergence of momentum-dependent spin textures – a variation of the spin direction over the Brillouin zone. At interfaces with trigonal crystal symmetries, these spin textures can also induce a non-zero Berry curvature even if magnetic order is absent[5–7]. The presence of SOC and Berry curvature in two dimensions is of significant importance for spintronics[8–10] and topological phenomena[11], respectively. Moreover, recent studies have shown that both SOC and Berry curvature are fundamental physical ingredients for HHG: the former governs terahertz third-harmonic generation in transition metals[12], while a direct correspondence between the latter and second-harmonic generation has been established in spin-orbit-free systems[13–16].

A relevant question is whether and how Berry curvature and SOC cooperate in non-centrosymmetric 2D materials for HHG, particularly in the context of even-order harmonics. Recent studies on the nonlinear Hall effect with time-reversal symmetry[7, 17–20] have established a close connection between SOC, Berry curva-

ture, and second-harmonic generation using a semiclassical approach[21]. The aim of this Letter is to demonstrate, using HHG selection rules[22] and explicit calculations, the interplay between SOC, quantum geometry, and high-order harmonics in 2D non-centrosymmetric systems, with a focus on the relation between the emergence of non-zero even-order harmonics and distinct symmetry-allowed spin textures. Note that in certain magnetic materials, non-zero second-order response has been attributed to distinctive magnetic patterns both with[23, 24] and without[25, 26] SOC, but without accounting for the contribution of the Berry curvature and the symmetry properties of the spin texture. Our analysis establishes that a spin texture that breaks a  $\hat{C}_2$  twofold rotational symmetry is necessary for observing even-order harmonics. The Berry curvature imposes constraints only in time-reversal symmetric conditions: its non-vanishing is essential for the appearance of even-order harmonics. By contrast, when time-reversal symmetry is broken even-order harmonics can persist even in the complete absence of Berry curvature.

*Spin textures and HHG spectrum* — Due to SOC, spin and charge degrees of freedom, and therefore spin textures and high-harmonic response, are interconnected. In particular, both the pattern of the spin texture and high-order harmonics are dictated by the point-group symmetries of the system under investigation: these are unitary operators  $\hat{P}$  that commute with the Hamiltonian  $\hat{H}_0$  of the system in the absence of external sources[27]. Assuming there is no residual  $\mathcal{U}(1)$  spin symmetry – which is equivalent to stating that the horizontal mirror symmetry is broken – a 2D system of spin-1/2 fermions can exhibit two distinct types of point-group symmetries. These correspond to proper rotations with respect to the out-of-plane ( $z$ ) axis, and vertical mirrors. Additionally, the system can be equipped with time-reversal (TR) symmetry. Here, we examine the impact of these symmetries on both spin textures and high-order harmonics. In particular, HHG is studied in the case of an external light

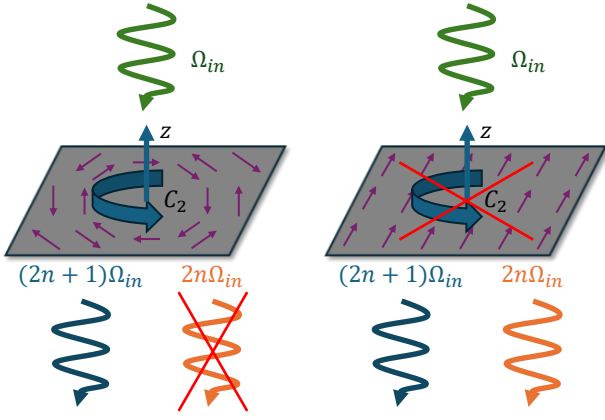


Figure 1. Illustration of spin-texture patterns in momentum space for high-harmonic generation. Left: in 2D systems with spin textures invariant under twofold rotational symmetry,  $\hat{C}_2$ , there is no emission of even-order harmonics. Right: for spin textures breaking  $\hat{C}_2$  symmetry, the emission of even-order harmonics is allowed.

pulse polarized in the in-plane direction, along which the system is space-periodic and the 2D crystal momentum  $\mathbf{k} \equiv (k_x, k_y, 0)$  is a good quantum number. The optical response of the system, associated with the current density  $\mathbf{J}(t) \equiv (J_x(t), J_y(t), 0)$ , can be obtained by incorporating the external vector potential  $\mathbf{A}(t)$ , which is related to the electric field  $\mathbf{E}(t)$  via  $\mathbf{E}(t) = -\partial_t \mathbf{A}(t)$  in the velocity gauge, into  $\hat{H}_0$ . This is accomplished using the Peierls substitution  $\mathbf{k} \rightarrow \mathbf{k} + \mathbf{A}(t)$  (where  $e = c = 1$  for simplicity)[22]. The details about the computation of  $\mathbf{J}$  are provided in the Supplemental Material [28]. Our focus is now on the system's general response under a monochromatic driving field  $\mathbf{A}(t) = \text{Re}\{\mathbf{A}_0 \exp(i\Omega t)\}$  oscillating with frequency  $\Omega$  or period  $T = 2\pi/\Omega$ , with  $\mathbf{A}_0$  the polarization vector: for linearly-polarized light it is  $\mathbf{A}_0 \propto (\cos\theta, \sin\theta, 0)$ , with  $\theta$  the polarization angle, while  $\mathbf{A}_0 \propto (2)^{-1/2}(1, \pm i, 0)$  if light is left/right-hand circularly-polarized. Owing to the time-periodicity of the external probe, the resulting time-dependent Hamiltonian,  $\hat{H}(t)$ , and the current density,  $\mathbf{J}(t)$ , are also time-periodic. This allows for the Fourier expansion

$$\mathbf{J}(t) = \sum_n \mathbf{J}_n e^{in\Omega t}, \quad (1)$$

where the Fourier component  $\mathbf{J}_n$  encodes the information on the emission of the  $n$ -th-order harmonic. The time-dependent Hamiltonian  $\hat{H}(t)$  is generally not invariant under the *static* point-group symmetry  $\hat{P}$ . As we show in details in [28], one must find a suitable combination of the point-group symmetry and an operator acting on the time variable. This combined symmetry, referred to as *dynamical* symmetry[22, 29–31], must ensure that both the momentum and the vector potential transform identically. Consider, for instance, the  $\hat{C}_2$  symmetry operation, which rotates the system by  $\pi$  around

the  $z$  axis, resulting in a sign flip of both momentum and spin. The sign flip of  $\mathbf{k}$  can be compensated by applying the time-translation operator  $\hat{T}_{T/2} = \exp\left(i\frac{T}{2}\partial_t\right)$ , which shifts time by half a period and thereby reverses the sign of the vector potential. Consequently, the combined operator  $\hat{g} \equiv \hat{C}_2 \otimes \hat{T}_{T/2}$  serves as a dynamical symmetry of the time-dependent Hamiltonian. In general, a dynamical symmetry  $\hat{g} \equiv \hat{P} \otimes \hat{T}_\tau$  that includes a time translation by a generic interval  $\tau$  imposes the following constraint on the  $n$ -order current

$$P\mathbf{J}_n = e^{i\Omega\tau} \mathbf{J}_n^{(*)}, \quad (2)$$

where  $P$  is the  $2 \times 2$  matrix associated with the action of  $\hat{P}$  on the two components of the current. Eq. (2) is valid when  $\hat{P}$  is (anti-)unitary, and its derivation is discussed in [28]. Here, we focus on its consequences. For  $\hat{C}_2$ -symmetric materials illuminated by monochromatic light, whether linearly or circularly polarized,  $\tau = T/2$  represents half the period and  $P = -1$  corresponds to minus the  $2 \times 2$  identity. As a result,

$$\hat{H}_0 \text{ is } \hat{C}_2\text{-invariant} \implies \mathbf{J}_n = (-1)^{n+1} \mathbf{J}_n. \quad (3)$$

Eq. (3) leads to the crucial consequence that, for even  $n$ ,  $\mathbf{J}_n$  vanishes. Beside, we recall that, as a consequence of the  $\hat{C}_2$ -invariance, the spin texture  $\sigma_{\mathbf{k}} \equiv \langle \hat{\sigma} \rangle_{\mathbf{k}}$  transforms as follows:

$$\hat{H}_0 \text{ is } \hat{C}_2\text{-invariant} \implies \begin{cases} \sigma_{-\mathbf{k}}^{xy} = -\sigma_{\mathbf{k}}^{xy} \\ \sigma_{-\mathbf{k}}^z = \sigma_{\mathbf{k}}^z \end{cases}. \quad (4)$$

Eqs. (3) and (4), whose key messages are illustrated in Fig. (1), constitute the first central result of this paper: in a 2D non-centrosymmetric system where the spin texture is  $\hat{C}_2$ -invariant the emission of even-order harmonics is forbidden. This important criterion implies that systems with  $\hat{C}_2$ -broken spin texture can, in principle, emit even-order harmonics. Before discussing this class of materials, we note that the one-to-one correspondence between the HHG selection rules and the spin texture in the presence of SOC holds a more general validity. To provide another example, we consider systems with a generic rotational invariance  $\hat{C}_N$  with respect to the angle  $\phi = 2\pi/N$ , where  $N = 2, 3, 4, 6$ , under a circularly-polarized pump field. In this case, the dynamical symmetry is  $\hat{g} \equiv \hat{C}_N \otimes \hat{T}_{T/N}$ , and as discussed in detail in [28], it imposes the constraint  $Q_N \mathbf{J}_n = \exp(i2\pi/N) \mathbf{J}_n$ , where  $Q_N$  is the matrix associated with the rotation of  $2\pi/N$ . Apart from the phase factor arising from the time-dependence of the driven Hamiltonian, the last equation closely resembles the corresponding constraint on the spin texture, which is  $Q_N \sigma_{\mathbf{k}} = \sigma_{Q_N \mathbf{k}}$ . These equations once again highlight the close connection between spin textures and high-order harmonics. When considering vertical mirrors, they impose constraints on the polarization of the harmonics. Here, we focus on a representative

result for a pump field that is linearly polarized perpendicular to a vertical mirror, while referring to [28] for a comprehensive analysis of the entire set of cases. Denoting  $\mathbf{J}^{\parallel}$  and  $\mathbf{J}^{\perp}$  as the components of the optical current parallel and perpendicular, respectively, to the mirror direction, we have

$$\begin{cases} \mathbf{J}_n^{\parallel} = \mathbf{0}, & n \text{ even,} \\ \mathbf{J}_n^{\perp} = \mathbf{0}, & n \text{ odd.} \end{cases} \quad (5)$$

This can be compared to the corresponding transformation of the spin texture,  $\sigma_{\mathbf{k}_{\parallel}, -\mathbf{k}_{\perp}}^{\parallel} = -\sigma_{\mathbf{k}_{\parallel}, \mathbf{k}_{\perp}}^{\parallel}$  and  $\sigma_{\mathbf{k}_{\parallel}, -\mathbf{k}_{\perp}}^{\perp} = \sigma_{\mathbf{k}_{\parallel}, \mathbf{k}_{\perp}}^{\perp}$ . From this point onward, we focus on even-order harmonics. Having identified the  $\hat{C}_2$ -invariant spin texture as a sufficient condition for their suppression, we now examine scenarios where spin textures break this symmetry, enabling their emission. In this context, it is essential to distinguish between the two cases in which TR symmetry is either preserved or broken.

*Systems with broken  $\hat{C}_2$  and preserved TR symmetry* We consider the spin texture and high-harmonic response of a TR-invariant trigonal lattice with threefold rotational symmetry ( $\hat{C}_3$ ) that explicitly breaks  $\hat{C}_2$  symmetry. The Hamiltonian is given by  $\hat{H}_0 = \varepsilon_{\mathbf{k}} \hat{\sigma}_0 + \mathbf{h}_{\mathbf{k}} \cdot \hat{\sigma}$ , where  $\hat{\sigma}_0$  is the identity matrix and  $\hat{\sigma}$  represents the Pauli matrices. Here, having defined  $\mathbf{a}_{1/2} = \pm (\sqrt{3}/2) \hat{x} - (1/2) \hat{y}$  and  $\mathbf{a}_3 = \hat{y}$ ,  $\varepsilon_{\mathbf{k}} = -2t [\cos(\mathbf{a}_1 \cdot \mathbf{k}) + \cos(\mathbf{a}_2 \cdot \mathbf{k}) + \cos(\mathbf{a}_3 \cdot \mathbf{k})]$  is the tight-binding energy dispersion,  $h_{\mathbf{k}}^{(x)} = -\gamma_R \boldsymbol{\eta}_{\mathbf{k}} \cdot \hat{y}$  and  $h_{\mathbf{k}}^{(y)} = \gamma_R \boldsymbol{\eta}_{\mathbf{k}} \cdot \hat{x}$ , with  $\boldsymbol{\eta}_{\mathbf{k}} = 2 [\mathbf{a}_1 \sin(\mathbf{a}_1 \cdot \mathbf{k}) + \mathbf{a}_2 \sin(\mathbf{a}_2 \cdot \mathbf{k}) + \mathbf{a}_3 \sin(\mathbf{a}_3 \cdot \mathbf{k})]$ , describe Rashba spin-momentum locking, and  $h_{\mathbf{k}}^{(z)} = 2\lambda [\sin(\mathbf{a}_1 \cdot \mathbf{k}) + \sin(\mathbf{a}_2 \cdot \mathbf{k}) + \sin(\mathbf{a}_3 \cdot \mathbf{k})]$  is the trigonal warping term. While the Rashba coupling is invariant under any rotation,  $h_{\mathbf{k}}^{(z)}$  breaks  $\hat{C}_2$ , reflecting the  $\hat{C}_3$  symmetry of the underlying lattice, and preserves a vertical mirror along the  $x$  axis, see Fig. (2)(a). It also generates a non-zero Berry curvature,  $\boldsymbol{\Omega}(\mathbf{k}) \propto \lambda[7]$ . The spin texture and the HHG spectrum for this system are presented in panels (b) and (c) of Fig.(2), respectively. Here, the HHG spectrum is computed under a monochromatic light pulse linearly-polarized along the  $y$  axis, which is orthogonal to the mirror axis. Even-order harmonics exhibit finite amplitude, consistent with the expectation from the spin texture shown in Fig. (2)(b), which breaks  $\hat{C}_2$ . These harmonics eventually vanish when the  $\hat{C}_2$ -breaking warping term approaches zero at  $\lambda = 0$  (see panel (c) and inset therein). Additionally, we observe that odd- and even-order harmonics are polarized perpendicular and parallel to the mirror axis, i.e., respectively, along the  $y$  and  $x$  axes. This is in agreement with the HHG selection rules in Eq. (5) for a pump field oriented perpendicular to a vertical mirror. It is relevant now to consider the fate of even-order

harmonics in a system with broken  $\hat{C}_2$  symmetry but zero Berry curvature. An example of such a system is one characterized by Rashba coupling and  $h_{\mathbf{k}}^{(z)} = \zeta k_x$ , where  $\boldsymbol{\Omega}(\mathbf{k}) = \mathbf{0}$  throughout momentum space. Explicit calculations demonstrate that, in this case, even-order harmonics vanish. This serves as a particular example of a more general result, as shown in [28]: in TR-invariant systems where the Berry curvature is zero throughout the momentum space, the emission of even-order harmonics is forbidden. Therefore, we conclude that, in 2D non-centrosymmetric materials with TR symmetry, a spin texture that breaks  $\hat{C}_2$  symmetry, combined with a finite Berry curvature, ensures the non-vanishing of even-order harmonics.

*Systems with broken  $\hat{C}_2$  and T-symmetry* — To show that even-order harmonics can effectively probe  $\hat{C}_2$ -breaking magnetic patterns in systems with broken inversion and TR symmetry, we examine the case of a square crystal that is intrinsically invariant under  $\hat{C}_2$  symmetry, but exhibits an antiferromagnetic spin arrangement and a charge imbalance (Fig. 2(d)) within the sub-lattice that together break the twofold rotational symmetry. The Hamiltonian reads  $\hat{H}_0 = \varepsilon_{\mathbf{k}}^{\mu} \hat{\tau}_{\mu} \otimes \hat{\sigma}_0 + h_{\mathbf{k}}^{\mu i} \hat{\tau}_{\mu} \otimes \hat{\sigma}_i$ , where  $\hat{\tau}_{\mu}$  are Pauli matrices representing sub-lattice degrees of freedom. To ensure  $\hat{C}_2$  symmetry breaking, we assume a finite charge imbalance  $\Delta\varepsilon$  within the sub-lattice,  $\varepsilon_{\mathbf{k}}^z = \Delta\varepsilon$ , and an antiferromagnetic pattern with a local magnetic field  $B$  oriented along the  $\hat{y}$  direction,  $h_{\mathbf{k}}^{zy} = B$ , as illustrated in Fig. 2(d). We also include Rashba coupling,  $h_{\mathbf{k}}^{xx} = -\gamma_R \sin k_y$  and  $h_{\mathbf{k}}^{yx} = \gamma_R \sin k_x$ . The resulting spin texture breaks rotational invariance, as clear from Fig. 2(e), and even-order harmonics become non-zero, as demonstrated in Fig. 2(f). These harmonics eventually vanish in the limit of zero charge imbalance, as indicated in the inset of Fig. 2(f), since the antiferromagnetic pattern alone is  $\hat{C}_2$ -invariant. As a concluding remark, we address the role of Berry curvature in enabling even-order harmonics when TR symmetry is broken. In this case, the spin texture may exhibit invariance under  $\hat{C}_2$ , thereby ensuring the vanishing of even-order harmonics, while the Berry curvature remains finite. An example of this scenario is a 2D ferromagnet with Rashba coupling and spin alignment along the out-of-plane direction. This case illustrates that, in the absence of TR symmetry, the rotational symmetry of the spin texture is the key factor in the emission of even-order harmonics.

*Conclusions* — We have investigated the interplay between spin textures, Berry curvature, and HHG in two-dimensional non-centrosymmetric systems. Our analysis reveals that the presence or absence of even-order harmonics is closely tied to the symmetries of the spin texture. Specifically, we established that spin textures with broken twofold rotational symmetry are essential for the emission of even-order harmonics. Furthermore, we demonstrated the crucial role of Berry curvature in

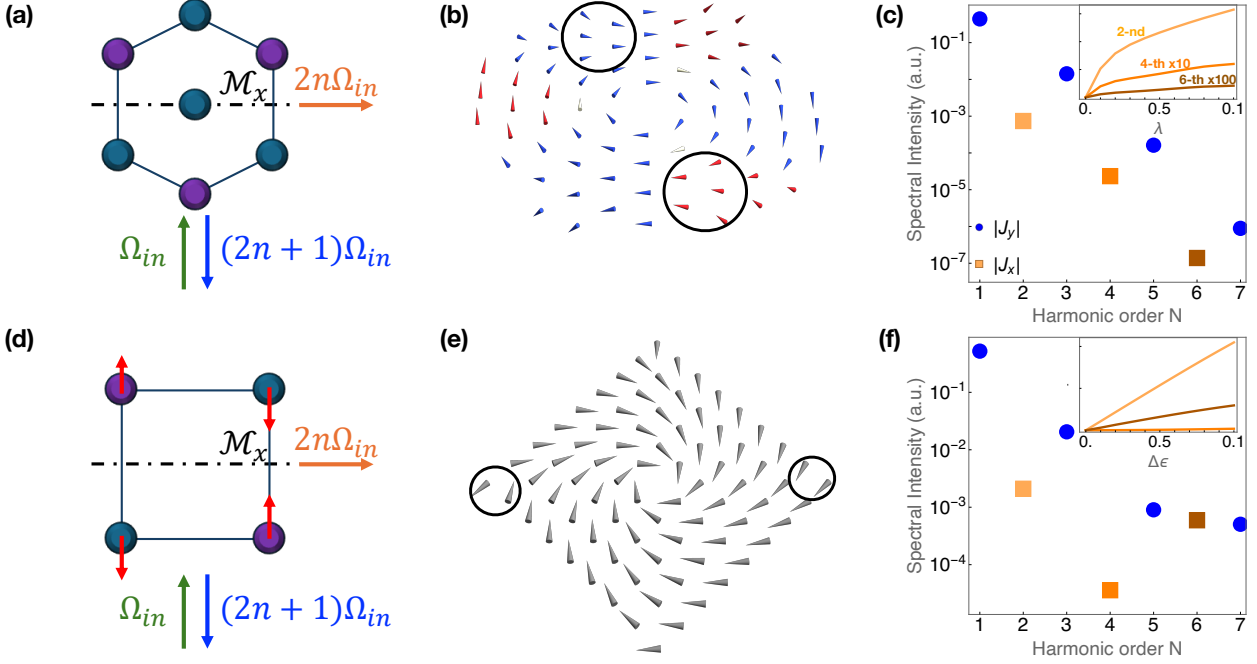


Figure 2. Spin textures and high-harmonic response for different physical configurations. Schematic illustration of the trigonal lattice (a) with threefold rotational symmetry and antiferromagnetic pattern (d) with broken twofold rotational symmetry. Both systems possess a vertical mirror symmetry  $\mathcal{M}_x$  along the  $x$ -axis, and in both cases, the incident field (green arrow) is polarized perpendicular to this direction. Blue and orange arrows represent the expected polarizations for odd- and even-order harmonics, respectively. Panels (b) and (e) show the spin textures in momentum space corresponding to the physical configuration in (a) and (d), respectively. The color legend indicates the out-of-plane spin component  $\langle \sigma_z \rangle$ , with color blue, gray and red corresponding to  $\langle \sigma_z \rangle = -1, 0$  and  $1$ , respectively. Black circles mark spots in the spin textures where  $\hat{C}_2$  symmetry, as described by Eq. (4), is broken. Panels (c) and (f) show the HHG spectra (in logarithmic scale) for the time-reversal-invariant trigonal configuration and the antiferromagnetic pattern, respectively. The Hamiltonian parameters, in units of the hopping energy  $t$ , are:  $\gamma_R = 0.1$  for both cases;  $\lambda = 0.1$  in (c); and  $\Delta\epsilon = 0.1$ ,  $B = 0.1$  in (f). The computations were performed at temperature  $T = 0$  with chemical potential  $\mu = 1.0$ . In both cases, the incident field has intensity  $|\mathbf{A}_0| = 1.0$  and frequency  $\Omega_{in} = 0.5$ . Polarizations of odd- (blue dots) and even-order (orange squares, with different shades of orange) harmonics are consistent with the outcomes of Eq. (5). The insets show the intensity of even-order harmonics (in linear scale) as functions of the parameters controlling the  $\hat{C}_2$ -symmetry breaking: the trigonal warping  $\lambda$  in (c) and the charge imbalance  $\Delta\epsilon$  in (f). The units and color legend of even-order harmonics in each inset are consistent with those of the corresponding panel.

enabling even-order harmonics in systems with time-reversal symmetry. We emphasize that rotational symmetry can be broken across various degrees of freedom, all linked to the high-harmonic response through spin-orbit interaction. This means that even-order harmonics can identify not only crystalline and spin patterns lacking rotational symmetry but also emergent electronic orderings with spatial reconstructions, such as in kagome systems, where trimerization breaks six-fold rotational symmetry[32]. Moreover, nontrivial high-harmonic response can also occur in systems exhibiting specific patterns of spin [33, 34] and orbitally polarized currents. Our results can also be applied to investigate spin ordering in low-dimensional altermagnets [35], marked, for specific terminations, by surface spin textures with odd-parity multipole patterns that break twofold rotational symmetry. All these rotational symmetry breakings, and the associated phase transitions, can be observed through

the shift from zero to finite even-order harmonic amplitudes, or conversely, when twofold symmetry is restored from a lower symmetry state.

### Acknowledgements

We acknowledge valuable discussions with Jeroen van den Brink. F.F. and F.G. acknowledge support from the Italian Ministry of University and Research (MUR) under Grant PRIN No. 2020JZ5N9M (CONQUEST) and under the National Recovery and Resilience Plan (NRRP), Call PRIN 2022, funded by the European Union - NextGenerationEU, Mission 4, Component 2, Grant No. 2022TWZ9NR (STIMO)-CUP B53D23004560006. M.C. acknowledges partial support from the EU Horizon 2020 research and innovation program under Grant Agreement No. 964398 (SUPERGATE) and, together with F.F., from NRRP MUR project PE0000023-NQSTI. C.O. acknowledges support by the Italian Ministry of Foreign Affairs and International Cooperation, Grant

No. PGR12351 (UTLRAQMAT) and the NRRP MUR project PE0000023-NQSTI (TOPQIN).

- 
- [1] S. Ghimire, A. D. DiChiara, E. Sistrunk, P. Agostini, L. F. DiMauro, and D. A. Reis, Observation of high-order harmonic generation in a bulk crystal, *Nature physics* **7**, 138 (2011).
- [2] H. A. Hafez, S. Kovalev, J.-C. Deinert, Z. Mics, B. Green, N. Awari, M. Chen, S. Germanskiy, U. Lehnert, J. Teichert, Z. Wang, K.-J. Tielrooij, Z. Liu, Z. Chen, A. Narita, K. Mullen, M. Bonn, M. Gensch, and D. Turchinovich, Extremely efficient terahertz high-harmonic generation in graphene by hot dirac fermions, *Nature* **561**, 507 (2018).
- [3] E. Rashba, Properties of semiconductors with an extremum loop. i. cyclotron and combinational resonance in a magnetic field perpendicular to the plane of the loop, *Sov. Phys.-Solid State* **2**, 1109 (1960).
- [4] G. Dresselhaus, Spin-orbit coupling effects in zinc blende structures, *Phys. Rev.* **100**, 580 (1955).
- [5] D. Xiao, M.-C. Chang, and Q. Niu, Berry phase effects on electronic properties, *Rev. Mod. Phys.* **82**, 1959 (2010).
- [6] M. T. Mercaldo, C. Noce, A. D. Caviglia, M. Cuoco, and C. Ortix, Orbital design of Berry curvature: pinch points and giant dipoles induced by crystal fields, *npj Quantum Materials* **8**, 12 (2023).
- [7] E. Lesne, Y. G. Saglam, R. Battilomo, M. T. Mercaldo, T. C. van Thiel, U. Filippozzi, C. Noce, M. Cuoco, G. A. Steele, C. Ortix, *et al.*, Designing spin and orbital sources of Berry curvature at oxide interfaces, *Nature Materials* **22**, 576 (2023).
- [8] A. Soumyanarayanan, N. Reyren, A. Fert, and C. Panagopoulos, Emergent phenomena induced by spin-orbit coupling at surfaces and interfaces, *Nature* **539**, 509 (2016).
- [9] K. Premasiri and X. P. Gao, Tuning spin-orbit coupling in 2D materials for spintronics: a topical review, *Journal of Physics: Condensed Matter* **31**, 193001 (2019).
- [10] A. Manchon, H. C. Koo, J. Nitta, S. M. Frolov, and R. A. Duine, New perspectives for Rashba spin-orbit coupling, *Nature Materials* **14**, 871 (2015).
- [11] Y. Ren, Z. Qiao, and Q. Niu, Topological phases in two-dimensional materials: a review, *Reports on Progress in Physics* **79**, 066501 (2016).
- [12] R. Salikhov, M. Lysne, P. Werner, I. Ilyakov, M. Schuler, T. V. A. G. de Oliveira, A. Ponomaryov, A. Arshad, G. L. Prajapati, J.-C. Deinert, P. Makushko, D. Makarov, T. Cowan, J. Fassbender, J. Lindner, A. Lindner, C. Ortix, and S. Kovalev, Spin-orbit interaction driven terahertz nonlinear dynamics in transition metals, *npj Spintronics* **3**, 3 (2025).
- [13] T. T. Luu and H. J. Wörner, Measurement of the Berry curvature of solids using high-harmonic spectroscopy, *Nature communications* **9**, 916 (2018).
- [14] H. Avetissian and G. Mkrtchian, High laser harmonics induced by the Berry curvature in time-reversal invariant materials, *Physical Review B* **102**, 245422 (2020).
- [15] Z. Lou, Y. Zheng, C. Liu, Z. Zeng, R. Li, and Z. Xu, Controlling of the harmonic generation induced by the Berry curvature, *Optics Express* **29**, 37809 (2021).
- [16] L. Yue and M. B. Gaarde, Characterizing anomalous high-harmonic generation in solids, *Physical Review Letters* **130**, 166903 (2023).
- [17] C. Ortix, Nonlinear Hall effect with time-reversal symmetry: Theory and material realizations, *Advanced Quantum Technologies* **4**, 2100056 (2021).
- [18] I. Sodemann and L. Fu, Quantum nonlinear hall effect induced by Berry curvature dipole in time-reversal invariant materials, *Phys. Rev. Lett.* **115**, 216806 (2015).
- [19] P. Makushko, S. Kovalev, Y. Zabala, I. Ilyakov, A. Ponomaryov, A. Arshad, G. L. Prajapati, T. V. A. G. de Oliveira, J.-C. Deinert, P. Chekhonin, I. Veremchuk, T. Kosub, Y. Skourski, F. Ganss, D. Makarov, and C. Ortix, A tunable room-temperature nonlinear Hall effect in elemental bismuth thin films, *Nat. Electron.* **7**, 207 (2024), 2310.15225.
- [20] Q. Ma, S.-Y. Xu, H. Shen, D. MacNeill, V. Fatemi, T.-R. Chang, A. M. Mier Valdivia, S. Wu, Z. Du, C.-H. Hsu, S. Fang, Q. D. Gibson, K. Watanabe, T. Taniguchi, R. J. Cava, E. Kaxiras, H.-Z. Lu, H. Lin, L. Fu, N. Gedik, and P. Jarillo-Herrero, Observation of the nonlinear hall effect under time-reversal-symmetric conditions, *Nature* **565**, 337 (2019).
- [21] J. Orenstein, J. Moore, T. Morimoto, D. Torchinsky, J. Harter, and D. Hsieh, Topology and symmetry of quantum materials via nonlinear optical responses, *Annual Review of Condensed Matter Physics* **12**, 247 (2021).
- [22] M. Lysne, Y. Murakami, M. Schüler, and P. Werner, High-harmonic generation in spin-orbit coupled systems, *Physical Review B* **102**, 081121 (2020).
- [23] M. Fiebig, V. V. Pavlov, and R. V. Pisarev, Second-harmonic generation as a tool for studying electronic and magnetic structures of crystals, *JOSA B* **22**, 96 (2005).
- [24] Z. Sun, Y. Yi, T. Song, G. Clark, B. Huang, Y. Shan, S. Wu, D. Huang, C. Gao, Z. Chen, *et al.*, Giant nonreciprocal second-harmonic generation from antiferromagnetic bilayer CrI<sub>3</sub>, *Nature* **572**, 497 (2019).
- [25] R.-C. Xiao, D.-F. Shao, W. Gan, H.-W. Wang, H. Han, Z. Sheng, C. Zhang, H. Jiang, and H. Li, Classification of second harmonic generation effect in magnetically ordered materials, *npj Quantum Materials* **8**, 62 (2023).
- [26] L. Šmejkal, A. H. MacDonald, J. Sinova, S. Nakatsuji, and T. Jungwirth, Anomalous Hall antiferromagnets, *Nature Reviews Materials* **7**, 482 (2022).
- [27] M. S. Dresselhaus, G. Dresselhaus, and A. Jorio, *Group theory: application to the physics of condensed matter* (Springer Science & Business Media, 2007).
- [28] In this Supplemental Material, we outline the computation of the optical current and discuss the crucial role of Berry curvature in enabling even-order harmonics in systems with time-reversal symmetry. Additionally, we provide further details on the symmetry properties of the time-dependent Hamiltonian and their implications for spin textures and high-order harmonics.
- [29] T. Janssen, A. Janner, and E. Ascher, Crystallographic groups in space and time: I. general definitions and basic properties, *Physica* **41**, 541 (1969).
- [30] O. E. Alon, V. Averbukh, and N. Moiseyev, Selection rules for the high harmonic generation spectra, *Physical review letters* **80**, 3743 (1998).
- [31] O. Neufeld, D. Podolsky, and O. Cohen, Floquet group theory and its application to selection rules in harmonic generation, *Nature communications* **10**, 405 (2019).
- [32] H. Zhang, B. D. Oli, Q. Zou, X. Guo, Z. Wang, and L. Li,

- Visualizing symmetry-breaking electronic orders in epitaxial kagome magnet FeSn films, *Nature Communications* **14**, 6167 (2023).
- [33] J. Wang, B.-F. Zhu, and R.-B. Liu, Second-order nonlinear optical effects of spin currents, *Phys. Rev. Lett.* **104**, 256601 (2010).
- [34] L. K. Werake and H. Zhao, Observation of second-harmonic generation induced by pure spin currents, *Nature Physics* **6**, 875 (2010).
- [35] S. G. Jeong, I. H. Choi, S. Nair, L. Buiarelli, B. Pourbahari, J. Y. Oh, N. Bassim, A. Seo, W. S. Choi, R. M. Fernandes, T. Birol, L. Zhao, J. S. Lee, and B. Jalan, Altermagnetic polar metallic phase in ultra-thin epitaxially-strained RuO<sub>2</sub> films (2024), arXiv:2405.05838 [cond-mat.mtrl-sci].